Electronic structure and polarons in $CaMnO_{3-\delta}$ single crystals: Optical data

N. N. Loshkareva, L. V. Nomerovannaya, E. V. Mostovshchikova, A. A. Makhnev, Yu. P. Sukhorukov, N. I. Solin, T. I. Arbuzova, S. V. Naumov, and N. V. Kostromitina
Institute of Metal Physics, 620219 Ekaterinburg, Russia

A. M. Balbashov and L. N. Rybina
Moscow Power Engineering Institute, 105835 Moscow, Russia
(Received 9 June 2004; revised manuscript received 4 October 2004; published 7 December 2004)

The ellipsometry measurements (in the energy range $E=0.5-5.0$ eV) on cleavage surfaces of single crystals, the measurements of the absorption and reflectance spectra ($E=0.04-0.8$ eV), electrical resistivity, and magnetic susceptibility were carried out for determination of peculiarities of the fundamental absorption spectrum and the conductivity mechanism in $CaMnO_{3-\delta}$ single crystals. The energy of fundamental absorption edge associated with the direct transitions was determined as $E_g=1.55$ eV. The absorption band with two maxima at 2.2 and 3.1 eV corresponding to the charge transfer transitions was revealed. The polaron band at 0.7 eV was discovered and polaron parameters were determined. Peculiarities of IR absorption and dc conductivity of $CaMnO_{3-\delta}$ in dependence on oxygen stoichiometry are determined by the superposition of hopping and band conductivity of spin-lattice polarons, and by additional localization of charge carriers under oxygen vacancies ordering.

DOI: 10.1103/PhysRevB.70.224406 PACS number(s): 75.47.Lx

I. INTRODUCTION

The manganites $La_{1-x}Ca_xMnO_3$ are objects under intensive study due to the "colossal magnetoresistance" for compositions with $0.17 \leqslant x \leqslant 0.50$ and $x \sim 0.9$.[1] Hole-doped manganites (with $x<0.5$) were synthesized and widely investigated both in polycrystalline and single-crystal form, see, for example, Ref. 2. Properties of manganites with electron-doping ($x>0.5$) were studied using only polycrystalline samples (see Refs. 3 and 4 and references in there). In Ref. 5 the data are reported about $CaMnO_3$ single crystals up to 0.5 mm maximum size grown from $CaCl_2$ fluxes, but any information about their optical properties is absent.

Experimental study of the electron structure of the manganites is the important fundamental problem. The questions about applicability of different approaches to description of ground and excited states are discussed in the literature: in what case it is necessary to take into account Coulomb repulsion on site for d electrons, what is the relative position of Mn($3d$) and O($2p$) bands, what is the nature of the charge gap. Optical properties give fundamental information about the energy spectrum of compound and are often used as a criterion of applicability of various methods for calculations of the electron structure. At the present time the question about the nature of low-energy excitations and existence of polarons in electron-doped manganites remains also unsolved. To find answers for all these questions, it is necessary to get experimental optical data on qualitative single crystals in a wide spectral range.

Optical conductivity spectra $\sigma(E)$ of $CaMnO_3$ polycrystalline samples were obtained in Refs. 6 and 7 from reflectivity spectra by the Kramers-Kronig transformation. Note that application of this method does not allow to find a fine structure of the optical spectra.

In the present work the ellipsometry measurements on cleavage surfaces of $CaMnO_{3-\delta}$ single crystals were performed in visible and near-infrared (IR) ranges to get spectra of the real and imaginary parts of permittivity. The optical absorption and reflection spectra of single-crystal plates were studied in the middle IR range. The goal of the present study is the determination of peculiarities of the fundamental absorption spectrum and interaction of light with the charge carriers in $CaMnO_{3-\delta}$ single crystals. X-ray diffraction, temperature dependence of electrical resistivity, magnetization, and paramagnetic susceptibility were investigated also.

In the paper the influence of oxygen nonstoichiometry of $CaMnO_{3-\delta}$ crystals on optical properties and dc resistivity are studied. The crystals grown in different atmosphere (air or argon) were used.

We show that there is the band in the optical conductivity spectra with two maxima at 2.2 and 3.1 eV, which can be associated with superposition of the charge-transfer transitions $O(2p) \rightarrow Mn(e_g)\uparrow$ and $O(2p) \rightarrow Mn(t_{2g})\downarrow$. Intensity of the peak at 2.2 eV depends on Mn contents. Earlier the band at 2.2 eV was not revealed in the optical conductivity spectra of $CaMnO_3$ polycrystalline samples.[6,7] Comparison experimental spectra of the optical conductivity in the visible range with the $\sigma(E)$ spectrum of $CaMnO_3$ obtained in Ref. 8 on the basis of local spin-density approximation (LSDA) band-structure calculations reveals substantial discrepancy of spectra both in the energy position of the fundamental bands and in distribution of the spectral weight. The energy of fundamental absorption edge corresponding to the direct transition is determined as $E_g=1.55$ eV. The band at ~ 0.7 eV found in the absorption and optical conductivity spectra is associated with lattice polarons. The higher-than-theoretical value of the effective magnetic moment in the paramagnetic range indicates that these polarons are spin-lattice ones. The variation of absorption coefficient and electrical resistivity of $CaMnO_{3-\delta}$ single crystals grown in different atmosphere is explained by different concentration of oxygen vacancies and their ordering.

TABLE I. Composition in weight and the atmosphere under the crystal growth; a is the parameter of pseudocubic lattice at $T=300$ K, T_C is the Curie temperature, θ is the paramagnetic Curie temperature, μ_{eff} is effective magnetic moment in μ_B.

Sample	Composition	a, nm	T_C, K	θ, K	μ_{eff}, μ_B
1	$CaMnO_3$ in Ar	0.7459 ± 0.0002	123	$-(385 \pm 5)$	4.15 ± 0.02
2	$CaMnO_3$ in air	0.7460	121	−415	4.37
3	$CaMnO_3$+1% Mn in Ar	0.7461	121	−270	3.95
4	$CaMnO_3$+1% Mn in air	0.7461	121	−370	4.24

II. SAMPLES AND EXPERIMENTAL DETAILS

Single crystals of $CaMnO_{3-\delta}$ were grown by a floating-zone method associated with an image furnace of URN-2-ZM type operated in different atmosphere in the Moscow Power Engineering Institute. The original polycrystalline samples were prepared by solid-state reaction of stoichiometric amounts of $CaCO_3$ and Mn_3O_4. The primary synthesis was carried out at $T=1100$ °C during 10 h. Obtained ceramics were grinded, sifted, and compacted by pressing in cylindrical feed rods. The final rods sintering was performed at $T=1250$ °C during 10 h. The single crystals were grown at the rate of 9.5 mm/h. The crystal annealing furnace temperature in the crystal growth run was about 1000 °C. Immediately after crystal growing the crystals were annealed at 1000 °C during 3 h additionally with the followed slow cooling. Two crystals were grown in argon (N1 and N3, see Table I). Another two crystals were grown in air (N2 and N4). For the crystal N2 grown in Ar and crystal N4 grown in air before the beginning of synthesis, 1% of Mn beyond the stoichiometric amount was added in mixture of the reactants. It was supposed that a crystal lost Mn during growth via some evaporation from the melt surface, and the addition of 1% Mn could enhance the manganese stoichiometry.

X-ray-diffraction studies showed the single crystals to be single phase. The parameters of the pseudocubic lattice of the crystals are given in Table I.

The refractive index n and absorption constant k were measured by the Beatty method on an automatic ellipsometer with the angle of incidence of 67° for the light over the spectral interval from 0.5 to 5 eV at room temperature with errors of 2–4%. The values of n and k were used to calculate the real $\varepsilon_1=n^2-k^2$ and imaginary $\varepsilon_2=2nk$ parts of the complex permittivity, reflectivity $R=[(n-1)^2+k^2]/[(n+1)^2+k^2]$, the optical conductivity $\sigma=nk\omega/2\pi$, the absorption coefficient $\alpha=2k\omega/c$ where ω is the angular frequency of the light wave. The samples for these measurements had sizes of $(3-5)\times 5\times 5$ mm^3. Cleavage surfaces and mechanically polished surfaces were used for ellipsometry measurements. The surfaces were cleaved along the direction of the crystal growth.

The absorption and reflection spectra in infrared range (0.04–0.60 eV) were studied using a high-sensitive automatic spectrometer. The thickness of polished plates of the single crystals was of 35–50 μm.

The temperature dependence of dc resistivity was recorded using the standard four-probe method in the temperature range 77–300 K. The magnetic measurements were carried out using Faraday magnetic balance within a temperature range of 80–600 K.

III. RESULTS AND DISCUSSION

A. Transport and magnetic properties of $CaMnO_{3-\delta}$ single crystals

The negative sign of the thermopower points out that at room temperature all studied single crystals are n-type semiconductors. Figure 1 presents the temperature dependence of dc resistivity $\rho(T)$ of the single crystals. The crystal N1 grown in Ar has the greatest value of ρ. The addition of 1% Mn decreases the resistivity of the crystals grown both in Ar and in air. The value of the resistivity at room temperature reported for polycrystalline samples of $CaMnO_3$ differs significantly in the literature. It is connected with the deviation from the oxygen stoichiometry. In nominally stoichiometic $CaMnO_3$ all Mn ions are Mn^{4+}. The oxygen vacancies in $CaMnO_3$ lead to the appearance of Mn^{3+} ions. When $\delta=0.5$ in $CaMnO_{3-\delta}$, all the Mn ions become trivalent.[5] The variation of oxygen contents in our samples was achieved by different atmosphere at the crystal growth and by addition of Mn in a part of samples (Table I). Because the argon is the reducing atmosphere, it is natural to expect that the amount of oxygen vacancies and, consequently, the amount of donors should be larger in crystal N1 grown in argon than in N2 grown in oxidizing air atmosphere. Then, the dc resistivity of the crystals grown in Ar should be less than that of crystals grown in air. However, the opposite picture is observed. The crystal N1 grown in Ar has the greatest value of ρ over all temperature range (Fig. 1). This fact can be understood on the basis of Ref. 9. Electron microscopy data reported in Ref. 9 show that when δ is changed from 0 to 0.5 different superstructures associated with the oxygen vacancies ordering are observed. Probably, a larger value of the resistivity of the crystal N1 with larger concentration of donors is a result of their stronger localization near ordered vacancies than in the crystal N2. The break of monotonous reduction of the dc resistivity value of $CaMnO_{3-\delta}$ ceramic samples versus oxygen vacancies concentration δ was observed at $\delta=0.16$ in Ref. 10 and associated with the vacancies ordering. Unexpectedly, the decrease of single-crystal resistivity occurs under the addition of 1% Mn (Fig. 1). Thus the 1% Mn addition does not give the improvement of manganese stoichiometry but, additionally, it increases the concentration of Mn^{3+} ions (by ~4%).

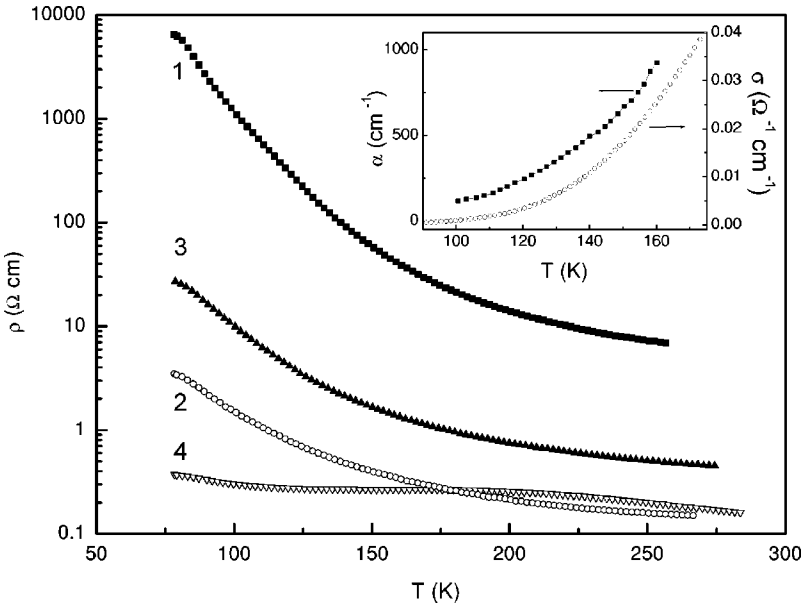

FIG. 1. Temperature dependence of the dc resistivity of the $CaMnO_{3-\delta}$ single crystals with different stoichiometry. The numbers of the samples at the curves correspond to that in Table I. The inset shows the temperature dependence of the dc conductivity and the absorption coefficient at the energy of 0.21 eV for the crystal N1.

The temperature dependence of the dc resistivity of $CaMnO_{3-\delta}$ single crystals in the temperature range 80–300 K in coordinates $\ln(\rho)$ vs $(10^3/T)$ is not described by linear dependence with single activation energy. However, for the crystals N1, N2, N3 there are linear regions in the dependence $\ln(\rho)$ vs $(1/T)^{1/4}$ at the temperatures below 130 K that indicates hopping conductivity with variable hopping length.

The temperature dependence of the magnetization M of $CaMnO_{3-\delta}$ single crystals in weak magnetic field (100 Oe) has the same behavior of $M(T)$ as for $CaMnO_3$ ceramic in Ref. 11: the rise of M is observed below $T \approx 125$ K. The Curie temperature T_C estimated by the beginning of the abrupt magnetization growth coincides for all studied crystals (see Table I). The crystal grown in Ar has a somewhat larger value of T_C. The negative paramagnetic Curie temperature for all crystals (Table I) obtained by extrapolation of Curie-Weiss-type linear dependence of paramagnetic susceptibility $\chi(T)$ $[\chi = C/(T+\theta)]$ in the interval 300–600 K indicates the dominant antiferromagnetic (AFM) exchange. The values of the effective magnetic moment of $CaMnO_{3-\delta}$ single crystals obtained from the temperature dependence of paramagnetic susceptibility $\chi(T)$ exceeds the theoretical value $\mu_{theor} = 3.87\mu_B$ (Table I). It indicates the retention of the ferromagnetic correlations up to 600 K, probably, due to the clusters with a large magnetic moment (spin polarons), see below. The direct relation between magnitudes of T_C and dc resistivity is absent. Probably, it is connected with strong competition between AFM superexchange and FM double exchange in nonstoichiometric $CaMnO_{3-\delta}$.

B. Optical properties of $CaMnO_{3-\delta}$ in visible and near IR range, connection with the electronic structure

Let us compare the optical properties of $CaMnO_{3-\delta}$ single crystals grown under different conditions. Figure 2 demonstrates $\sigma(E)$ spectra of $CaMnO_{3-\delta}$ single crystals grown in Ar and air and measured both on cleavage surfaces and on mechanically polished surfaces. The optical conductivity spectrum of all crystals shows the main band of the intensive interband absorption in the range of 1.0–4.5 eV with two maxima at 2.2 and 3.1 eV. In the near-IR range there is a comparatively weak absorption band at ~0.7 eV. As it is seen from Fig. 2, the intensity of the main absorption band for the crystal N1 is greater by 25%, and the minimum at ~1.0 eV is deeper than for the crystal N2. The addition of 1% Mn results in a small decrease of the intensity of the subband at 2.2 eV and a rise of absorption at the energy below 1.1 eV.

The mechanical polishing of the crystal surface by the diamond powder with the grain size of 0.5–1.0 μm does not decrease the intensity of the main absorption band. This fact agrees with the conclusion of Ref. 12 about insignificant influence of surface preparation manner on the optical spectra in the fundamental absorption range for the undoped manganite $LaMnO_3$. So, the spectral profile and the energy position of the main peculiarities of $\sigma(E)$ spectra in the range of the fundamental absorption band do not change significantly with variation of oxygen vacancies concentration δ and under different methods of preparation of mirror surfaces.

The higher quality of obtained spectra should be noted in comparison with Ref. 6. The intensity of our $\sigma(E)$ is spectra more than three times higher than $\sigma(E)$ spectra of polycrystalline samples in Ref. 6 obtained from reflection spectra using Kramers-Kronig transformation. Besides, in Ref. 6 the fine structure of the main band (peak at 2.2 eV) was not revealed.

The real $\varepsilon_1(E)$ and imaginary $\varepsilon_2(E)$ parts of permittivity of $CaMnO_{3-\delta}$ crystal N1 grown in argon are shown in the right inset in Fig. 2. The complicated form reflects abnormal dispersion in the range of strong interband absorption. The absorption band in the near-IR range (at ~0.7 eV) is best seen in $\varepsilon_2(E)$ spectra than in $\sigma(E)$ spectra. This band is observed for all samples. For the crystal N1 the band is resolved better although its intensity is lower than for other samples.

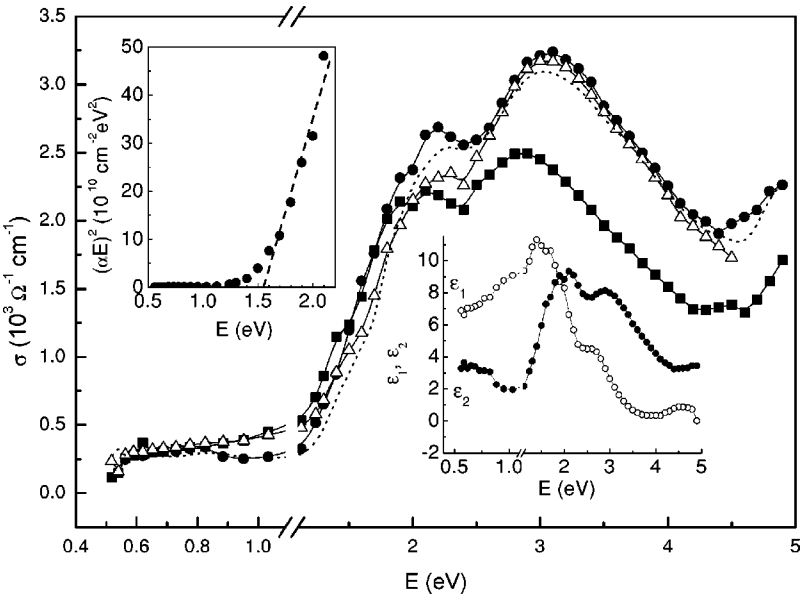

FIG. 2. Optical conductivity spectra of the $CaMnO_{3-\delta}$ single crystals with the different stoichiometry at room temperature. The symbols show the $\sigma(E)$ spectra obtained from the cleavage surface of crystal N1 (solid circles), N2 (solid squares), and N3 (open triangles); the dotted line is the $\sigma(E)$ spectrum for the $CaMnO_{3-\delta}$ crystal N1 with the polished surface. The right inset shows the real $\varepsilon_1(E)$ and imaginary $\varepsilon_2(E)$ parts of the permittivity of the crystal N1 obtained from the cleavage surface. The left inset shows dependence $(\alpha E)^2$ vs E for the $CaMnO_{3-\delta}$ crystal N1.

The dependence of $\alpha(E)^2$ versus photon energy E, where α is absorption coefficients, is shown in the left inset in Fig. 2 for crystal N1 in the absorption band edge region. The linear dependence is evidence that the absorption band edge is related to direct transitions. The energy of the direct transitions onset equals $E_g = 1.55$ eV. The optical gap of $CaMnO_3$ predicted from the electron structure calculations is $E_g > 0.42$ eV.[13] The nature of the band at ~ 0.7 eV in the forbidden gap will be considered below.

The electron structure calculations of $CaMnO_3$ with G-type AFM initial state had been performed in Refs. 8, 13, and 14. The electron configuration of the Mn^{4+} ion in $CaMnO_3$ is $(t_{2g}{}^3 e_g{}^0)$, i.e., all e_g states are empty, and therefore the cubic structure is stable. The Mn t_{2g} electrons are completely polarized. The density of oxygen p states extends throughout the region of 7 eV to the bottom of the gap and also appears through the hybridization in the conduction bands (see Fig. 3 in Ref. 13).

Let us compare the experimental and theoretical spectra of the optical conductivity (Fig. 3). The calculations of the optical conductivity for G-type AFM $CaMnO_3$ were performed within the local spin-density approximation (LSDA).[8] As it is seen from Fig. 3, calculation predicts two clearly defined absorption bands with maxima at 1.4 and 3.5 eV. The first (1.4 eV) peak corresponds to the charge-transfer transitions from the $O(2p)$ band to the $Mn(e_g)\uparrow$ and $Mn(t_{2g})\downarrow$ bands (see also Ref. 13). The second (3.5 eV) peak is due to the $O(2p) \rightarrow Mn(e_g)\downarrow$ excitations. Note that the energy interval occupied by the interband absorption in $\sigma(E)_{\text{theor}}$ is close to that in $\sigma(E)_{\text{expt}}$, but the magnitude of $\sigma(E)_{\text{theor}}$ is three times less than that of $\sigma(E)_{\text{expt}}$. It is seen that the low-energy part of $\sigma(E)_{\text{expt}}$ is shifted as compared with $\sigma(E)_{\text{theor}}$ in the direction of high energy by ≈ 0.3 eV. Besides, the essential spectral weight is "lost" on the theoretical curve in a wide energy range 1.5–3.5 eV.

According to analyses of optical conductivity spectra of $CaMnO_3$ polycrystalline sample[6] the peaks at 3.1 and 6.5 eV were assigned to $O(2p) - Mn(e_g)\uparrow$ and $O(2p) - Mn(e_g)\downarrow$ transitions, respectively. The energy difference be-

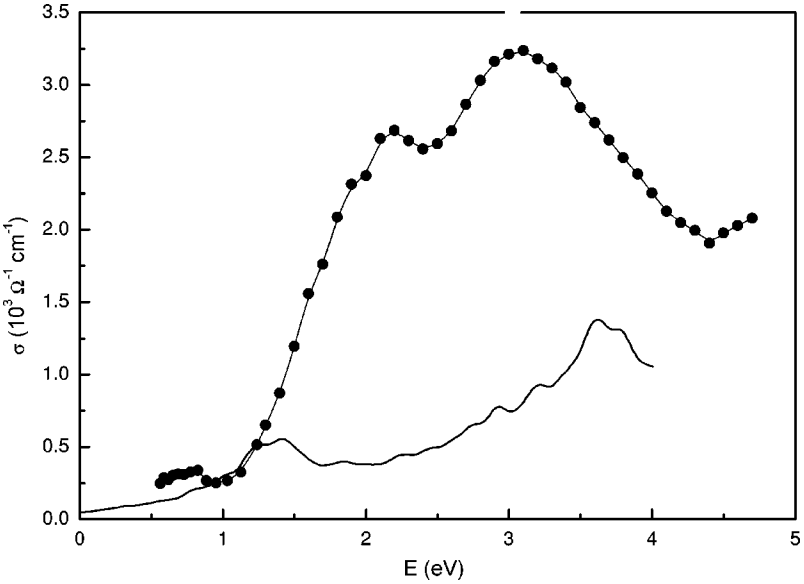

FIG. 3. Experimental optical conductivity spectrum (symbols) of the $CaMnO_{3-\delta}$ single crystal N1 in the comparison with the theoretical one (solid line) obtained on the basis LSDA calculation in Ref. 8.

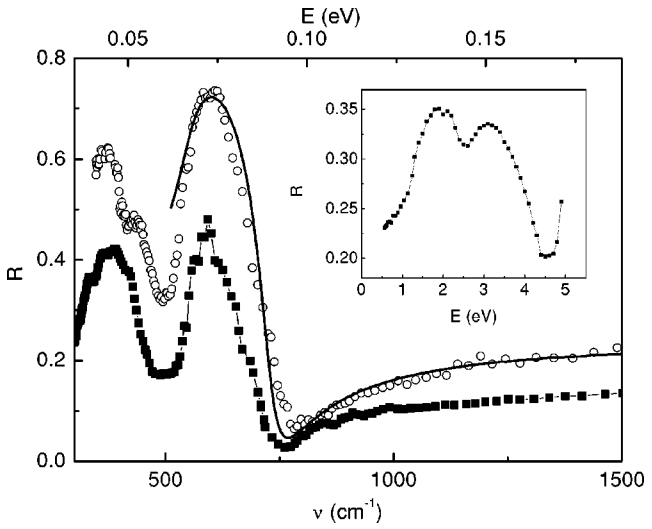

FIG. 4. Experimental reflection spectrum of $CaMnO_{3-\delta}$ crystal N2 grown in air (open circles) and the theoretical one (line), the reflection spectrum of $LaMnO_3$ single crystal (solid squares) at room temperature. The inset shows the reflection spectrum for the $CaMnO_{3-\delta}$ crystal N1 in the fundamental absorption range.

tween the second and the first peaks is determined by the Mn *d*-band exchange splitting ~3.0 eV for $CaMnO_3$.[13] In our case the two-peak band in energy interval 1.4–4.5 eV with small energy distance between peaks can be assigned to superposition of $O(2p) \rightarrow Mn(e_g)\uparrow$ and $O(2p) \rightarrow Mn(t_{2g})\downarrow$ transitions. The absorption rise above 4.5 eV is possibly the beginning of the band associated with $O(2p) \rightarrow Mn(e_g)\downarrow$ transition. The change of intensity of the peak at 2.2 eV, perhaps, is associated with the existence of Mn^{3+} ions in $CaMnO_{3-\delta}$ single crystals. More detailed theoretical calculations are necessary for unequivocal interpretation of the complex band.

C. Absorption of $CaMnO_{3-\delta}$ in middle IR range: Polarons

For determination of the conductivity mechanism and parameters of phonons of $CaMnO_{3-\delta}$, the reflection spectra $R(E)$ were studied. As an example, the experimental reflection spectrum of the crystal N2 measured at room temperature is shown in Fig. 4. For all crystals $R(E)$ spectra in IR range are similar: the depth of the minimum before the phonon spectrum and the value of the reflection in the range between phonon and fundamental spectra are close. The minimum before the phonon spectrum is rather deep, and the nondispersion range is wide. This character of $R(E)$ is similar to the one for wideband semiconductors with insignificant concentration of free charge carriers. When the charge-carriers concentration increases in wideband semiconductor abrupt plasma edge and plasma minimum appear in reflection spectra, and their energy position depends on concentration of free charge carriers. In our case dc conductivity (σ_{dc}) of crystals N3 and N4 is rather large, so the charge-carriers concentration is great, but plasma edge and plasma minimum are absent. $R(E)$ curves are close for $CaMnO_{3-\delta}$ crystals with different dc conductivity 0.16–6.3 $\Omega^{-1}\,cm^{-1}$ at room temperature. Such form of $R(E)$ spectra was observed for semiconductors with low mobility of charge carriers of polaron type, for example, ferrites and perovskite $BaTiO_3$.[15] For ferrites with dc conductivity 10^{-5}–1.8 $\Omega^{-1}\,cm^{-1}$ reflection spectra were almost independent versus the value of σ_{dc}. Even when the dc conductivity reached ~200 $\Omega^{-1}\,cm^{-1}$ in ferrites and perovskite $BaTiO_3$ the form of reflection spectra as a whole remained, the value of R in nondispersion range increased, but plasma minimum did not appear.[15] The similarity of reflection spectra of our crystals and $R(E)$ spectra in Ref. 15 gives evidence that $CaMnO_{3-\delta}$ crystals belong to the class of semiconductors with low-mobile charge carriers.

Figure 4 demonstrates theoretical $R(E)$ spectrum of $CaMnO_3$ calculated by formulas of dispersion analysis in the model of two independent oscillators.[16] The frequency of longitudinal high-frequency phonon mode $\nu_{LO}=742.7\ cm^{-1}$ needed for further estimation was found by fitting the theoretical curve R_{theor} to the experimental curve R_{expt}. Besides, the following phonon parameters were obtained: the frequency of transverse high-frequency mode $\nu_{TO}=514.6\ cm^{-1}$ and the damping parameter $\gamma=1.17\times10^{13}\ c^{-1}$.

As it is seen from Fig. 4, the initial part of the phonon spectrum in the reflection of $CaMnO_{3-\delta}$ single crystals is close to that of $LaMnO_3$. We assume that the phonon spectrum of $CaMnO_{3-\delta}$ and $LaMnO_3$ in the absorption spectrum $\alpha(E)$ will begin at the same energy.

Let us consider the optical-absorption spectra $\alpha(E)$ of $CaMnO_{3-\delta}$ single crystals. All $CaMnO_{3-\delta}$ crystals are opaque in the middle IR range at room temperature and become partially transparent only under cooling. Figure 5 demonstrates absorption spectra $\alpha(E)$ of $CaMnO_{3-\delta}$ crystals recorded at 85 K in comparison with the spectrum of $LaMnO_3$ single crystal from Ref. 17. The range of transparency of the crystal N1 is narrower than the one for $LaMnO_3$. Significant growth of α in $CaMnO_{3-\delta}$ occurs below 0.16 eV and above 0.3 eV. A comparison between reflection and absorption spectra (Figs. 4 and 5) points out that the phonon absorption of $LaMnO_3$ and $CaMnO_{3-\delta}$ begins below 0.1 eV. Therefore the absorption rise of $CaMnO_{3-\delta}$ below 0.16 eV is due to another process, probably to the interaction of light with free charge carriers. In the high-energy part of the spectral range, the increase of the $CaMnO_{3-\delta}$ absorption coefficient with the energy growth begins at lower energy (~0.3 eV) than that of $LaMnO_3$ (~0.4 eV). For $LaMnO_3$ the indirect band gap $E_g=0.41$ eV at 80 K was determined from the absorption spectrum in Ref. 17. For $CaMnO_{3-\delta}$ the absorption growth at the energy above 0.3 eV is not connected with the tail of the interband absorption. It is proved by estimate of the temperature shift of spectrum dE/dT for the crystal N2 grown in air, which was annealed in oxygen (Fig. 6). The value dE/dT for this crystal at the absorption coefficient of 1000 cm^{-1} is 1.2×10^{-3} eV/K. This magnitude is by an order of value greater than for the conventional shift of the fundamental absorption edge of a semiconductor. Therefore the absorption spectrum of $CaMnO_{3-\delta}$ at $E>0.3$ eV is associated with the tail of the band at 0.7 eV revealed by ellipsometry method (Fig. 2) and located below the fundamental absorption edge $E_g \approx 1.55$ eV.

As known, the light interaction with charge carriers dominates in a semiconductor in the range between the fundamen-

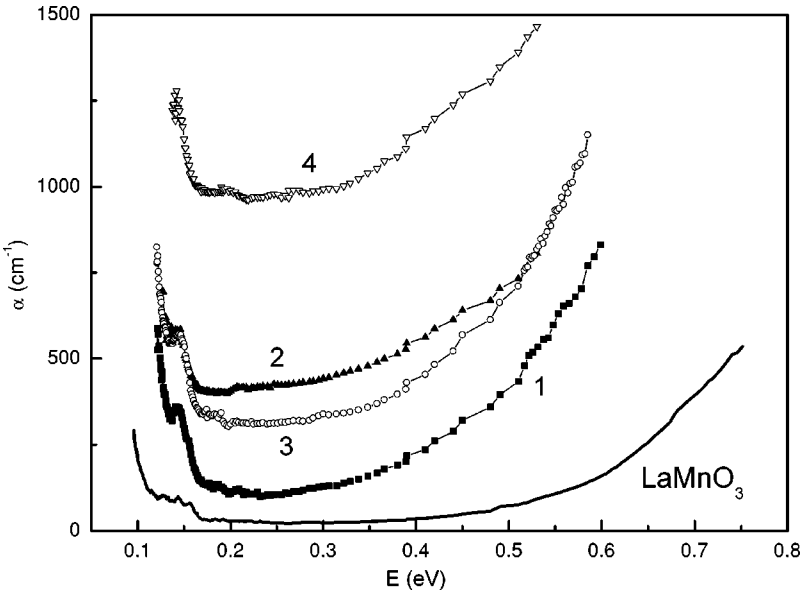

FIG. 5. Absorption spectra of the $CaMnO_{3-\delta}$ single crystals recorded at $T=85$ K. The numbers of the samples at curves correspond to that in Table I.

tal absorption edge and phonon spectrum. Comparison of optical properties in this spectral range and dc conductivity can give information about the mechanism of conductivity. As it is seen from Fig. 5, the crystal N1 with the greatest dc resistivity (the least dc conductivity) has the least absorption coefficient among all the crystals in the energy range 0.1–0.6 eV. Except the crystal N2, the absorption coefficient of the crystals at 85 K is more when the dc conductivity is more. All crystals are opague at room temperature as a result of the high density of donor states associated with Mn^{3+} ions, which appear due to the oxygen vacancies. It is in accordance with rather high value of dc conductivity (small resistivity, see Fig. 1). In the range above 0.6 eV this tendency of absorption change versus σ_{dc} remains. As follows from ellipsometry measurements at room temperature, when dc conductivity grows the intensity of the band at 0.7 eV in $\sigma(E)$ spectra increases from 305 $\Omega^{-1}\,cm^{-1}$ for crystal N1 to 350 $\Omega^{-1}\,cm^{-1}$ for crystal N3. Thus there is the same tendency of σ and α change versus dc conductivity of crystals in the whole IR range (0.12–1.1 eV). We note that change of optical absorption as well as that change of σ_{dc} with oxygen nonstoichiometry at room temperature is less than at 85 K.

Now we will consider the evolution of optical absorption with temperature. The temperature dependence of absorption coefficient $\alpha(T)$ for crystal N1 at the energy of 0.21 eV correlates with the temperature dependence of dc conductivity (inset in Fig. 1). Detailed measurement of absorption spectra at different temperatures was performed on crystal N2 grown in air and annealed in oxygen at 800 °C during 5 h (Fig. 6). An annealing of crystal in oxidizing atmosphere enhances oxygen stoichiometry, decreases the number of oxygen vacancies and, respectively, the donor concentration, and reduces the absorption coefficient (see for comparison Figs. 5 and 6). In the inset in Fig. 6 the temperature dependence of absorption at different energies is demonstrated. As it is seen from Fig. 6, the absorption coefficient rises under heating. The rate of growth $\alpha(T)$ is stronger in the low-energy range at 0.14 eV than in the high-energy one at 0.51 eV. It is

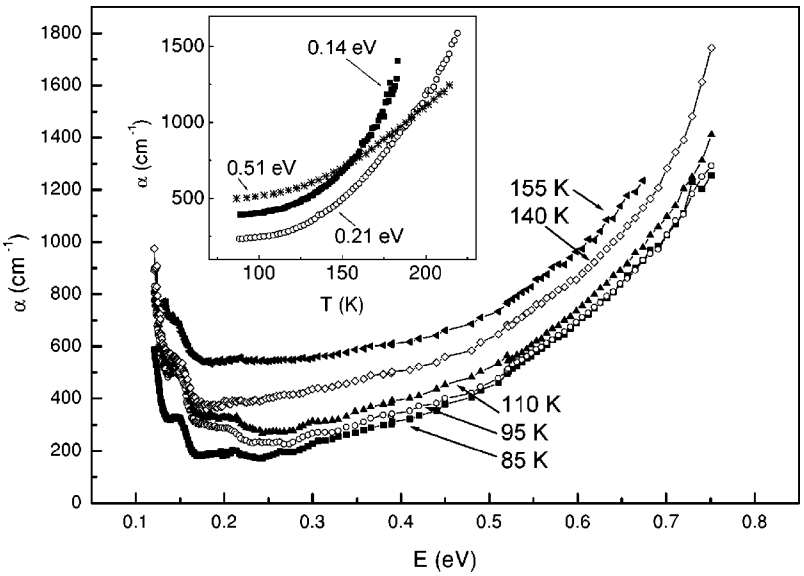

FIG. 6. Absorption spectra of the $CaMnO_{3-\delta}$ crystal grown in air (N2) and then annealed in O_2 recorded at different temperatures. The inset shows the temperature dependence of the absorption coefficient at different energies.

clearly seen from the inset in Fig. 6. The energy of 0.14 eV is related to the range where the interaction of light with free charge carriers occurs. The energy of 0.51 eV belongs to the tail of the band with maximum at $E=0.7$ eV. This different rate of α growth with temperature will be discussed below.

The typical view of the reflection spectrum for conducting materials with polaron conductivity, the correlation of the temperature dependences of the band intensity, and dc conductivity allows us to conclude that the band at 0.7 eV is associated with low-mobile charge carriers, namely, polarons. The polaron band had been predicted for slightly electron-doped $CaMnO_3$, and the excitation spectrum of the spin-lattice polaron had been calculated in Ref. 18. The polaron spectrum was located at the energy higher than ~2 eV. However, the authors of Ref. 18 expected a shift of the spectrum to the lower energy if a bigger number of electronic states should be used in calculations.

The energy position of the absorption band and connection of its intensity with dc conductivity are similar to corresponding characteristics for the polaron band of rutile TiO_2 described in classic works.[19,20] In accordance with the theoretical consideration of light interaction with small radius lattice polarons,[19] the energy of the polaron band maximum E_{max} is equal to $4E_a$ where E_a is the activation energy of polaron mobility. The value of $E_p=2E_a=A\hbar\omega_0$ is the polaron binding energy, A is the electron-phonon coupling parameter, ω_0 is the limiting phonon frequency. The binding energy E_p is the energy gain obtained by self-trapping of electrons in the crystal lattice.

The polaron parameters of our $CaMnO_{3-\delta}$ crystals are determined in the framework of the small-radius polaron model. The activation energy of the polaron is $E_a=0.175$ eV, the polaron binding energy is $E_p=0.35$ eV, the electron-phonon coupling parameter is $A=3.9$. For evaluation of A the foregoing experimental value of $\omega_0=2\pi c\nu_0$ was used, $\nu_0\equiv\nu_{LO}=742.7$ cm^{-1} ($\hbar\omega_0=0.09$ eV). The value of the polaron binding energy E_p is in a good accordance with $E_p=0.39$ eV obtained in Ref. 21 from the photoinduced absorption spectrum of $CaMnO_3$. This energy has been associated with photoinduced holes forming small polarons. The electron-phonon coupling parameter $A=3.9$ is typical for small-radius polarons.[15]

The width of the absorption band connected with the small polarons can be estimated from the formula $\Delta E=8\sqrt{(E_a\hbar\omega_0/2)}$ for the case of low temperatures $T\ll\hbar\omega_0$.[20] The obtained value of $\Delta E=0.7$ eV agrees quite well with the experimental width of the absorption band (Fig. 2).

From the maximal intensity of polaron band $\alpha(E_{max})$ the value σ_{dc} can be estimated according to the formula pointed out in Ref. 20,

$$\frac{\alpha(E_{max})}{\sigma_{dc}}=\frac{4\pi}{nc}\frac{kT}{E_{max}}\exp\left(\frac{E_{max}}{4kT}\right).$$

The estimate gives for the most conductive crystal N4 (with the absorption coefficient $\alpha=4.8\times10^4$ cm^{-1} at room temperature) the σ_{dc} value by an order of magnitude greater than the experimental one. Probably, it means that the dc conductivity is determined by not only polaron formation. The localization process connected with oxygen vacancies ordering and, consequently, polaron ordering could decrease the dc conductivity.

Our data show that at least two mechanisms of conductivity take place: polaron hopping and polaron band conductivity. The rates of absorption rise versus temperature are different near the tail of the polaron band (at $E=0.51$ eV; see the inset in Fig. 6) connected with the polaron hopping and near phonon spectrum (at $E=0.14$ eV) where the absorption reflects polaron band conductivity. The more abrupt dependence of $\alpha(T)$ at 0.14 eV than at 0.51 eV indicates that the change of the contribution of the polaron band conductivity is stronger than that of polaron hopping conductivity in the temperature range 130–180 K.

The reason for a weaker change of the intensity of the 0.7-eV band than dc conductivity with oxygen nonstoichiometry is connected with a different relation of contributions of polaron hopping and polaron band conductivity in dc conductivity and in high-frequency (optical) conductivity. For magnetite Fe_3O_4 dc conductivity has been also explained by the superposition of hopping conductivity and the band conductivity of the small-radius lattice polaron.[22] The main contribution to dc conductivity below 350 K was connected with polaron band conductivity, whereas the optical conductivity in the middle infrared range was determined by the polaron hopping conductivity.

Magnetic data show that all crystals are antiferromagnetic with weak ferromagnetic contribution (see Sec. III A). The higher-than-theoretical value of the effective magnetic moment in the paramagnetic range obtained from the paramagnetic susceptibility (Table I) gives evidence for ferromagnetic correlations caused by oxygen vacancies (donors). The donor electrons polarize magnetic moments of the nearest Mn ions and make a contribution in the polaron binding energy. Thus the polarons discussed above must be spin polarons. As it has been supposed in Ref. 23, below T_N polarons in $CaMnO_3$ interact one to another antiferromagnetically. It is seen from Fig. 6 that peculiarities in $\alpha(T)$ curves near the temperature of the magnetic phase transition (~120 K) are absent. Application of the magnetic field up to 8 kOe does not influence the optical absorption of $CaMnO_{3-\delta}$ crystals in the magnetic ordered range. It may be an evidence of magnetic hardness of polarons.

The following factors influence the spin-lattice polaron formation: localization due to electron-phonon coupling, oxygen vacancies ordering, and strong competition between AFM superexchange and FM double exchange.

IV. CONCLUSIONS

The study of optical properties of $CaMnO_{3-\delta}$ single crystals reveals the fundamental absorption band with two maxima at 2.2 and 3.1 eV. The energy of the fundamental absorption edge associated with the direct transitions was determined as $E_g=1.55$ eV. The polaron band at 0.7 eV was revealed. The comprehensive investigation of IR absorption, electrical resistivity, and magnetic susceptibility indicates

that the charge carriers in $CaMnO_{3-\delta}$ are spin-lattice polarons. The superposition of hopping and band conductivity of polarons and additional localization of charge carriers under oxygen vacancies ordering determine peculiarities of IR absorption and dc conductivity of $CaMnO_{3-\delta}$ in dependence on oxygen stoichiometry.

ACKNOWLEDGMENTS

The authors thank N. G. Bebenin and B. A. Gizhevskii for discussion. The work was supported by RFBR, Project No. 02-02-16429, and by the Department of Physical Sciences of RAS.

[1] C. Martin, A. Maignan, M. Hervieu, and B. Raveau, Phys. Rev. B **60**, 12191 (1999).
[2] G. Biotteau, M. Hennion, F. Moussa, J. Rodriguez-Carvajal, L. Pinsard, A. Revcovlevschi, Y. Mukovskii, and D. Shulyatev, Phys. Rev. B **64**, 104421 (2001).
[3] C. D. Ling, E. Granado, J. J. Neumeier, J. W. Lynn, and D. N. Argyriou, Phys. Rev. B **68**, 134439 (2003).
[4] E. Granado, C. D. Ling, J. J. Neumeier, J. W. Lynn, and D. N. Argyriou, Phys. Rev. B **68**, 134440 (2003).
[5] K. R. Poeppelmeier, M. E. Leonowicz, and J. M. Longo, J. Solid State Chem. **44**, 89 (1982).
[6] J. H. Jung, K. H. Kim, D. J. Eom, T. W. Noh, E. J. Choi, J. Yu, Y. S. Kwon, and Y. Chung, Phys. Rev. B **55**, 15489 (1997).
[7] J. H. Jung, K. H. Kim, T. W. Noh, E. J. Choi, and J. Yu, Phys. Rev. B **57**, R11043 (1998).
[8] I. Solovyev and K. Terakura, in *Electronic Structure and Magnetism of Complex Materials*, edited by D. J. Singh and D. A. Papaconstantopoulos (Springer, Berlin, 2003).
[9] A. Reller, J. M. Thomas, and D. A. Jefferson, Proc. R. Soc. London, Ser. A **394**, 223 (1984).
[10] J. Briatica, B. Alascio, R. Allub, A. Butera, A. Caneiro, M. T. Causa, and M. Tovar, Phys. Rev. B **53**, 14020 (1996).
[11] J. J. Neumeier and J. L. Cohn, Phys. Rev. B **61**, 14319 (2000).
[12] K. Takenaka, K. Iida, Y. Sawaki, S. Sugai, Y. Moritomo, and A. Nakamura, J. Phys. Soc. Jpn. **68**, 1828 (1999).
[13] W. E. Picket and D. J. Singh, Phys. Rev. B **53**, 1146 (1996).
[14] S. Satpathy, Z. S. Popovich, and F. R. Vikajlovic, J. Appl. Phys. **79**, 4555 (1996).
[15] M. I. Klinger and A. A. Samokhvalov, Phys. Status Solidi B **79**, 9 (1977); P. Gerthsen, R. Groth, and K. H. Hardtl, Phys. Status Solidi **11**, 303 (1965).
[16] A. A. Kukharskii, Opt. Spektrosk. **41**, 499 (1976) [Opt. Spectrosc. **41**, 290 (1976)].
[17] N. N. Loshkareva, Yu. P. Sukhorukov, E. V. Mostovshchikova, L. V. Nomerovannaya, A. A. Makhnev, S. V. Naumov, E. A. Gan'shina, I. K. Rodin, A. S. Moskvin, and A. M. Balbashov, Zh. Eksp. Teor. Fiz. **121**, 412 (2002) [JETP **94**, 350 (2002)].
[18] Y-R. Chen, V. Perebeinos, and B. Allen, Phys. Rev. B **65**, 205207 (2002).
[19] V. N. Bogomolov, E. K. Kudinov, D. N. Mirlin, and Yu. A. Firsov, Fiz. Tverd. Tela (Leningrad) **9**, 2077 (1967) [Sov. Phys. Solid State **9**, 1956 (1967)].
[20] V. N. Bogomolov and D. N. Mirlin, Phys. Status Solidi **27**, 443 (1968).
[21] T. Mertelj, M. Hrovat, D. Ku-aer, and D. Mihailovic, Int. J. Mod. Phys. B **14**, 3590 (2000).
[22] D. Ihler and B. Lorenz, J. Phys. C **19**, 5239 (1986).
[23] C. D. Batista, J. Eroles, M. Avignon, and B. Alascio, Phys. Rev. B **62**, 15047 (2000).